ISSN 1993-6842 (on-line); ISSN 0233-7657 (print)
Biopolymers and Cell. 2021. Vol. 37. N 6. P 447–458
doi: http://dx.doi.org/10.7124/bc.000A6A

UDC 577.336+577.112.7

Benzoxazole styrylcyanine dye as a fluorescent probe for functional amyloid visualization in *Staphylococcus aureus* ATCC25923 biofilm

S. V. Chernii[1], O. V. Moshynets[1], D. I. Aristova[1], D. V. Kryvorotenko[1], M. Yu. Losytskyy[1], O. S. Iungin[1,2], S. M. Yarmoluk[1], G. P. Volynets[1]

[1] Institute of Molecular Biology and Genetics, NAS of Ukraine
150, Akademika Zabolotnoho Str., Kyiv, Ukraine, 03143

[2] Kyiv National University of Technologies and Design
2, Nemirovich-Danchenko Str., Kyiv, Ukraine, 01011
chernii.sv@gmail.com

Aim. Synthesis and characterization of styrylcyanine dye as a potential fluorescent probe for the detection *in vitro* of pathological amyloid fibrils and functional amyloid in *S. aureus* biofilm. **Methods.** Chemical synthesis, fluorescence spectroscopy, irradiation with a visible light source, confocal laser scanning microscopy, fluorescence microscopy. **Results.** Styrylcyanine dye is low fluorescent when free, but in the presence of amyloid fibrils in vitro shows an increase in the emission intensity up to 214 times depending on the amyloidogenic protein structure; the most pronounced enhancement was observed for fibrils of beta-lactoglobulin. Photostability of the dye in the free state is low, but binding to amyloid fibrils results in a strong increase of dye photostability. Upon staining *S. aureus* biofilm, the dye stains extracellular components of the biofilm matrix and does not penetrate the cell. **Conclusion.** This dye is suggested to visualize the functional amyloids of *S. aureus* biofilm with a red emission.

Keywords: fluorescence microscopy, styryl dyes, *S. aureus*, functional amyloids, bacterial biofilm, laser scanning confocal microscopy.

Introduction

Biofilms are the natural aggregations of bacterial cells found when bacterial colonization takes place [1, 2]. Biofilm contributed to pathogenicity, survival, and persistence [3–5]. The known structure and functions of biofilm indicate that it is one of the most widespread and most successful life forms on Earth [6]. Biofilms offer bacteria several advantages: they constitute a protective physical barrier to nonspecific and specific host defenses during infection; they confer tolerance to antimicrobial agents (disinfectants and antibiotics) by reducing the diffusion of those toxic compounds, effectively reducing the grazing by

protozoa [7–10]. The protective benefits of biofilms depend on their inherent structure (matrix) and the gene expression patterns of sessile cells [9, 11]. The structural integrity of the biofilm depends upon the extracellular polymer substances (EPS) formed in the biofilm matrix produced by its constituent microorganisms [12]. The EPS of bacterial biofilms are complex mixtureof exopolysaccharides, nucleic acids, proteins, and other compounds [13–15]. Functional amyloids contribute to the matrix EPS of many Gram-positive and Gram-negative biofilms where they provide attachment, initial aggregation and, finally, biofilm matrix stabilization [16, 17].

Staphylococcus aureus is a virulent pathogen[, which is] currently the most common cause of infections in hospitalized patients [18]. *S. aureus* infection can involve any organ system and causes high morbidity and mortality due to endovascular complications and metastatic infections [19]. Although polysaccharides are the main structural element of the biofilm, the extracellular proteins significantly contribute to its functioning. Bap (biofilm-associated protein) is considered a virulence factor of *S. aureus* and promotes cell adhesion of the pathogen [20]. The BapB subunit formed by proteolytic cleavage of Bap is amyloidogenic and is involved in the formation of functional amyloids. Another identified amyloidogenic component of the *S. aureus* biofilm is phenol-soluble moduline (PSM). PSM lyses blood cells, induces immune responses, modulates the structure and development of the biofilm [21]. Sortase A might also contribute to the amyloidogenesis in *S. aureus* biofilms [22]. Functional amyloids play an essential role in the formation and functioning of biofilms and their stability, so there is a need to create tools to visualize bacterial biofilms and their amyloid component. Amyloid fibrils are usually determined by fluorescent methods. The main structural feature of amyloid aggregates is an ordered β-folded structure that provides specific binding of fluorescent probes. The methods for studying functional amyloids include fluorescence microscopy using the amyloid-sensitive dye Thioflavin T, several other fluorescent probes [23], antibody labeling [24], polarization microscopy using the dye Congo Red [25]. Noteworthy, for the BapB subunit of *S. aureus*, the formation of amyloid oligomers and fibrils was confirmed as well as their binding to the dyes Congo Red, Thioflavin T [26]. However, these dyes have disadvantages. In particular, Congo Red also binds cellulose and protein-binding factors, and Thioflavin has low reproducibility and specificity (and also binds to nucleic acids) [27].

Recently, we have reported the fluorescent sensitivity of β-ketoenole dyes to amyloid fibrils, both pathological and functional ones emitting in the green spectral range [28–30]. Specifically, these dyes have shown high sensitivity and were low-fluorescent when free and in the presence of native proteins and other essential structural components of biofilm matrix. However, they display strong green-yellow emission in the presence of amyloid fibrils.

This work aimed to study the amyloid-sensitive styrylcyanine dye (Scheme 1) as a red-emitted stain to visualize amyloid components of the extracellular matrix of bacterial biofilms. For this purpose, the *in vitro* fluorescent sensitivity of this dye to different biomolecules was studied. Specifically, we focused

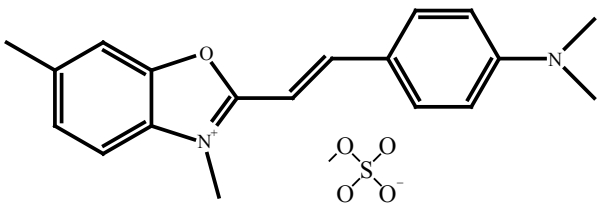

Scheme 1. Chemical structure of styryl dye D-16.

on the major components of cells, biofilm matrix EPS, and components of medium for cultivation, in particular, nucleic acids, polysaccharides, lipids, and proteins. Irradiation was performed to study the photostability of the dyes. The efficient visualization of amyloid-producing biofilm by styryl dye was explored on the model biofilm developed by *Staphylococcus aureus* ATCC25923 bacteria used by us previously [30]. To estimate the ability of the dye to penetrate cells and to stain intracellular components, the staining of human MCF-7 cells as an amyloid fibrils-free model was carried out.

Materials and Methods

Synthesis. A mixture of 0.002 mol of benzoxazole and 0.002 mol dimethylsulfate was heated for 1 h at 100 °C. 0.002 mol of 4-dimethylaminobenzaldehyde were added in 1 ml of n-butanole and refluxed for 1h. Water was added. Crystalline dye precipitate was filtered off and crystallized from ethanol.

Chemical analysis. The structure of synthesized dye was confirmed with ^{1}H NMR spectra and elemental analysis. Yield 37 % ; m.p. (dec.): > 200 °C ; ^{1}H NMR (DMSO d $_6$) δ (ppm):

^{1}H NMR (Varian Mercury VRX-400 spectrometer, 400 MHz): δ 8.17 (d, J = 15.3 Hz, 1H), 8.01 – 7.66 (m, 4H), 7.44 (d, J = 8.6 Hz, 1H), 7.30 (d, J =15.4 Hz, 1H), 6.82 (d, J = 8.5 Hz, 2H), 4.01 (s, 3H), 3.65 (d, J = 7.0 Hz, 3H), 3.08 (s, 6H).

Anal.calc. for C_{20} H_{26} N_2 O_5 S : C 59.09; H 6.45; N 6.89.Found : C 60.10; H 6.62; N 6.98.

BLG aggregation. *Beta*-lactoglobulin (Sigma-Aldrich) was dissolved at 5 mg/mL concentration in a water solution of HCl pH 2 or buffer pH 7. Fibrils were formed by incubating the protein solution in a Thermomixer incubator at 80 °C for 24 hours at pH 2 [31]. At pH 7, fibrils of BLG were formed by incubating the protein solution in a Thermomixer incubator at 65 °C for 24 h. The presence and shape of the fibrillar aggregates were confirmed by TEM.

Insulin aggregation. Human insulin (Sigma-Aldrich) was dissolved at 340 μM (2 mg/mL) concentration in 0.1 M water solution of HCl. Fibrils were formed by incubating the protein solution in a water bath at 65 °C for 5 hours [32]. The presence and shape of the fibrillar aggregates were confirmed by TEM.

Lysozyme aggregation. Hen eggs lysozyme (Sigma–Aldrich) was dissolved at 1 mM (14.5 mg/mL) concentration in 0.1 M water solution of HCl. Aggregates were formed by incubating the protein solution in a Thermomixer incubator at 65 °C for about 24 hours [25]. The presence and shape of aggregates were confirmed by TEM.

Spectral measurements. Fluorescence excitation and emission spectra were collected on a Cary Eclipse fluorescence spectrophotometer (Varian). The excitation light wavelength was equal to was equal to that of lowest-energy band maximum in the respective excitation

spectrum. All measurements were performed in standard 10 mm quartz cuvettes at room temperature.

Working solutions of free dye were prepared by diluting the dye stock solution with Tris-HCl buffer (pH 7.9) to the concentration of 5 μM (for all measurements). The working solutions of dye/protein mixtures were prepared by adding the aliquot of stock solution of monomer insulin or fibrillar insulin/lysozyme aggregates to the 5 μM dye solution. Insulin concentration in the working solution was 3.4 μM, lysozyme concentration in the working solution was 4 μM, BLG concentration in the working solution was 4 μM. The working solutions of dye/NA mixtures were prepared by mixing 5 μM of dye and an aliquot of DNA, low molecular DNA, or RNA stock solutions in Tris-HCl buffer (final concentration of dsDNA was 61.5 μM b.p. and RNA was 123 μM b.p.).

The working solution of the dye/BSA mixture was prepared by adding the dye to 3 μM BSA solution (dye concentration in the working solution was 5 μM). The working solution of dye/starch mixture was prepared by adding a starch aliquot to 5 μM working solution of dye (final starch concentration was 0.04 mg/ml). The working solution of dye/lecithin mixture was prepared by adding lecithin aliquot to 2 μM working solution of dye (final lecithin concentration was 0.04 mg/ml).

Dye photostability. Photostability of the dyes in solution and the presence of DNA were studied using the laboratory-designed equipment: the transparent glass vials with the samples (3 mL of each sample) were placed into the container with the reflecting inner surface. In contrast, the irradiating unit was installed on the top of the container. The irradiating unit consisted of 27 light-emitting diodes (blue light, 470 nm). The cool water was placed inside the container that served as a water bath to prevent the heating of the samples. The distance between the samples and the lamp was 2 cm. The photostability of the studied dye was estimated both in a free state and in the presence of amyloid fibrils or dsDNA (5 μM dye) in 50 mM Tris-HCl buffer (pH 7.9). After irradiation of the mentioned samples during a specific time (15, 30, 45, or 60 min), the irradiated solutions were placed into the quartz cell, absorption and fluorescence spectra of these solutions were measured, and the absorption values (A) were obtained. Photostability of the dyes was then characterized by the ratios A/A_0, where A_0 was the absorption of corresponding solutions prepared in the same way without irradiation. Photostability measurements were repeated three times for each sample, and standard deviations were calculated.

Bacteria, biofilm formation, and sample preparation. S.aureus ATCC 25923 strain was cultured aerobically at 37 °C in the classical Luria-Bertani (LB) medium shaking to provide inocula [33]. Overnight culture of the strain was used to produce biofilms in stationary LB microcosms containing 5 ml. *S.aureus* biofilms were obtained at 37 °C and harvested in three days. Solid-liquid biofilms formed onto a bottom surface of each microcosm were sampled and put on microscopic glass slides for the following staining with dyes SYBR Green and D-16.

Confocal Laser Scanning Microscopy analysis (CLSM). CLSM analysis was done using Leica TCS SPE Confocal system with

coded DMi8 inverted microscope (Leica, Germany). 5 μL of each dye was used to stain the samples. D-16 was used in the concentration of 10^{-3} M. The following concentrations of other dyes were used: AmyGreen solution contained 10^{-3} and SYBR Green (Invitrogen) solution corresponded to 100×, Ethidium Bromide solution contained 2 μg/ml. Images were acquired using excitation at 488 nm, emission collected at 501–595 nm for SYBR Green and AmyGreen and excitation at 532 nm and emission collected at 551–733 for the experimental dye D-16 and Ethidium bromide.

Cell culture cultivation. Human breast adenocarcinoma cell line MCF-7 was obtained from Bank of Cell Lines of the R. E. Kavetsky Institute of Experimental Pathology, Oncology and Radiobiology, NASU (Ukraine). The MCF-7 cells were cultivated in DMEM culture medium (Gibco, USA) supplemented with 10 % fetal bovine serum (FBS, HyClone, USA), 4 mM glutamine, 50 units/ml penicillin, 50 μg/ml streptomycin at 37 °C in the presence of 5 % CO2.

Fluorescence imaging of MCF-7 cells. For live-cell imaging, the growth medium was removed and the cells were washed twice by pre-heated PBS, after that the cells were incubated with styryl dye in FluoroBrite DMEM (Gibco, USA) without FBS for 30 min at 37 °C in the presence of 5 % CO_2. Then cells were rewashed with PBS and placed in FluoroBrite DMEM. The cells were fixed in 10 % neutral buffered formalin (Sigma-Aldrich, USA) for 15 min at 22 °C for microscopy of fixed cells. Cell membranes were permeabilized with 0.2 % Triton X-100 in PBS for 10 min at 22 °C. After that, cells were incubated with 10 mM cupric sulfate and 50 mM ammonium acetate, pH 5.0 for 30 min at 22 °C to reduce autofluorescence. Next, cyanine dyes in PBS were added to the samples for 30 min at 22 °C in the dark. Among all incubations, the cells were washed three times with PBS. In the end, the samples were embedded into Mowiol 4–88 mounting medium (Sigma-Aldrich, USA) containing 2.5 % DABCO (Sigma-Aldrich, USA). Microscopy image acquisition was performed using Leica DM 1000 epifluorescent microscope with an excitation filter of 515–560 nm and an emission filter of 580 nm for the dye D-16. The obtained images were analyzed using free software Fiji/ImageJ v1.52b [34].

Results and discussion

Study of the spectral-luminescent properties of the dye D-16 and its sensitivity to biomolecules

The specificity of the response of D-16 to amyloid fibrils was investigated comparing the response to fibrillar proteins *in vitro* with the response to other biomolecules: nucleic acids, albumin, starch (as a model polysaccharide), soybean lecithin, and BSA. Spectral-luminescent properties of the styrylcyanine dye in 50 mM Tris–HCl buffer solution (pH 7.9) are presented in Table 1. The studied dye possesses low fluorescence intensity in the free state and in the presence of native amyloidogenic proteins (insulin, BLG, lysozyme), BSA, scratch (up to 6 times), and soybean lecithin (up to 23 times). Fluorescence maxima of the dye are located in the green-yellow area of the spectrum (552–556 nm), while fluorescence excitation maxima are in the range 490–492 nm. The presence of amyloid fibrils of different proteins and nucleic acids results in

a significant increase in dye fluorescence intensity. The most significant spectral responses are observed for amyloid fibrils of BLG (214 times) following DNA, RNA (102 and 191 times, respectively), and amyloid fibrils of lysozyme (108 times). The dye binding also results in a red-shift of fluorescence emission and excitation maxima of the dye. The shift of the excitation maximum is up to 58 nm, and the shift of the emission maximum is up to 27 nm in the long-wavelength region. Thus, the dye exhibits fluorescent sensitivity to both amyloid fibrils and nucleic acids, depending on their type.

Table 1. **Spectral-luminescent properties of dye D-16**

	dye D-16			
	λ_{ex}	λ_{em}	I_f	I_f/I_0
free dye	490	552	2.5	-
mINS	490	554	2.0	-
fINS	532	576	240	96
mBLG	491	554	2.6	-
fBLG	532	579	535	214
mLYS	490	554	2.5	-
fLYS	522	559	270	108
BSA	490	555	10	4
DNA	525	560	254	102
lDNA	548	569	210	84
RNA	527	564	478	191
scratch	492	556	15	6
soybean lecithin	490	555	58	23

λ_{ex}, λ_{em} — maximum wavelength of excitation, emission spectrum, nm; I_f — fluorescence inyensity; I_f/I_0 — increase of fluorescent intensity (number of times, where I_0 — fluorescence intensity of free dye and I_f — fluorescence intensity of dye in the presence of biomolecules. *mINS* — monomeric insulin, *fINS* — amyloid fibrils of insulin, *mBLG* — monomeric beta-lactoglobulin, *fBLG* — amyloid fibrils of beta-lactoglobulin, *mLYS* — monomeric lysozyme, *fLYS* — fibrillar lysozyme, *BSA* — bovine serum albumin, *lDNA* — low molecular *DNA*, *DNA* — high molecular *DNA*.

Study of dye D-16 stability in the absence and in the presence of biomolecules

To investigate the relationship between styrylcyanine dye photostability in the free state and in the presence of amyloid fibrils (fBLG) or nucleic acids (dsDNA), we studied the effect of irradiation of the dyes solutions by the blue light (working wavelength about 470 nm) on the absorption spectra of these solutions. The changes in the characteristics of the absorption spectra of the dye (absorbance at wavelength maximum) after 15, 30, 45, and

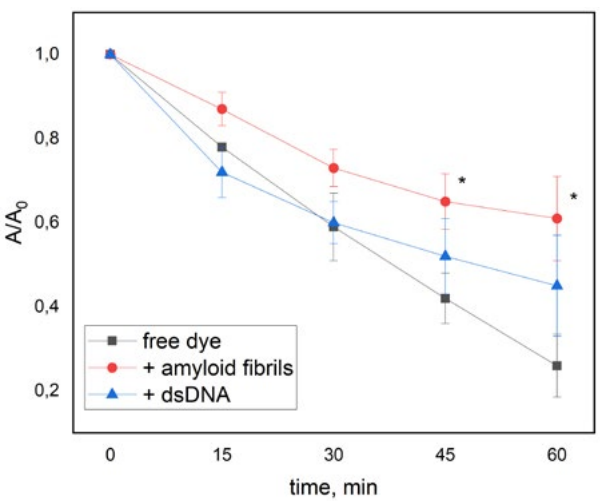

Fig. 1. Graphs of dependence of the ratio A/A_0 upon irradiation time (min), where A is the absorbance at maximum wavelength of the sample after irradiation during 0, 15, 30, 45, and 60 min, and A_0 is the optical density of the sample before irradiation, for dye D-16 in the free state (black), in the presence of amyloid fibrils (red) or dsDNA (blue). C_{dye} = 5 μM in 50 mM Tris-HCl buffer pH 7.9 (* — $p<0.05$).

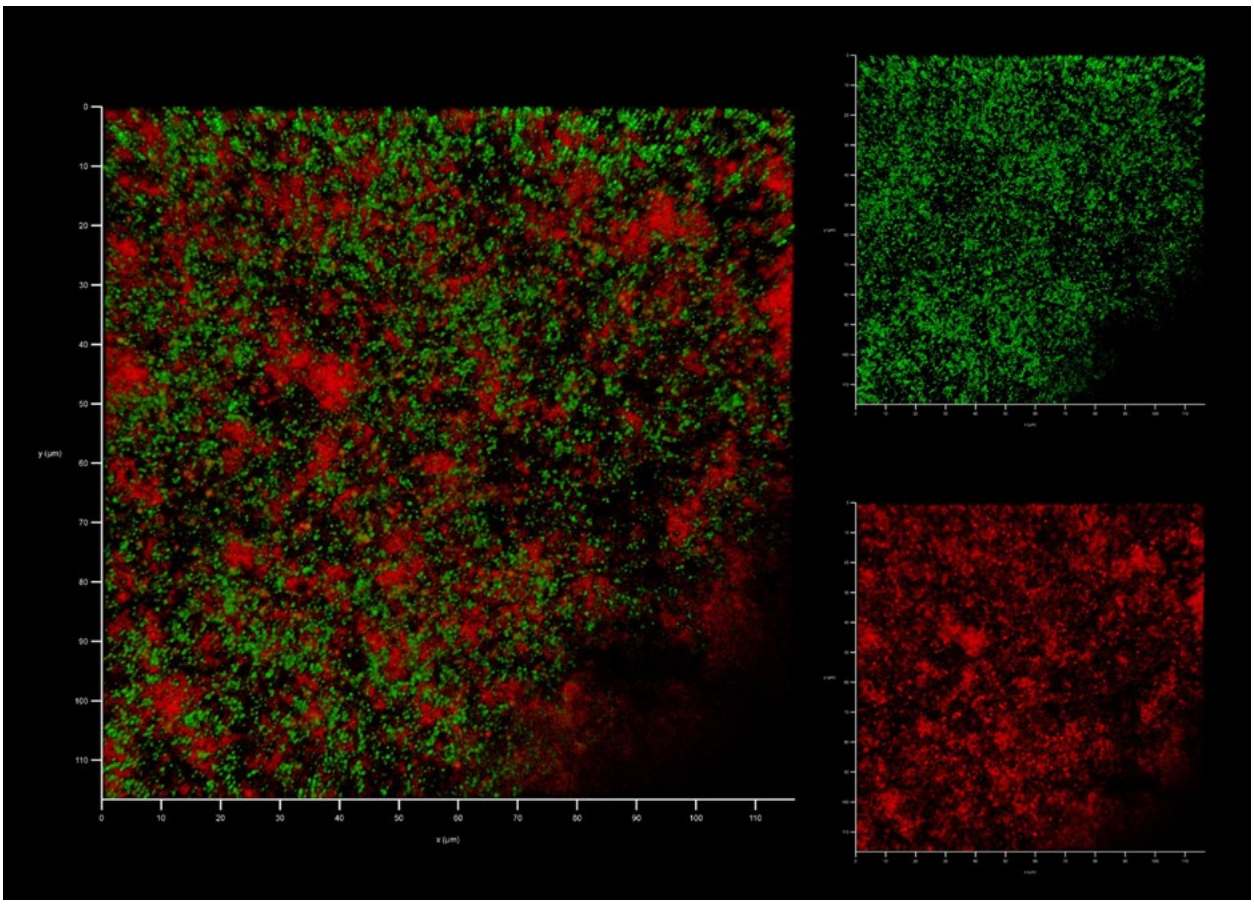

Fig.2. CLSM visualization of three-day-old biofilm of *S.aureus* ATCC 25923, co-stained by SYBR Green (green) to visualize intracellular DNA, i.e. bacterial cells, and dye D-16 (red) to visualize functional amyloids in the biofilm matrix.

60 minutes of irradiation are presented in Fig. 1.

It could be seen from Fig.1 that irradiation of the free dye solution leads to the photodestruction of the dye during 60 min. The presence of dsDNA and amyloid fibrils led to an increase in the photostability of the dye. Over the first 30 min, the photostability of the dye in the presence of nucleic acid does not differ from that in the free state. In the presence of amyloid fibrils, the photostability of the dye remains higher during all the time of the experiment. We suggest that an increase in the dye photostability should be due to its binding to biomolecules with a higher binding ability to amyloid fibrils of BLG. As a higher photostability of the dye in the presence of amyloid fibrils is observed, we studied the ability of the dye to visualize the components of the biofilm.

S. aureus ATCC25923 biofilm visualization by styrylcyanine dye

Biofilm of *S. aureus ATCC25923* bacteria was co-stained by D-16 and SYBR Green dyes

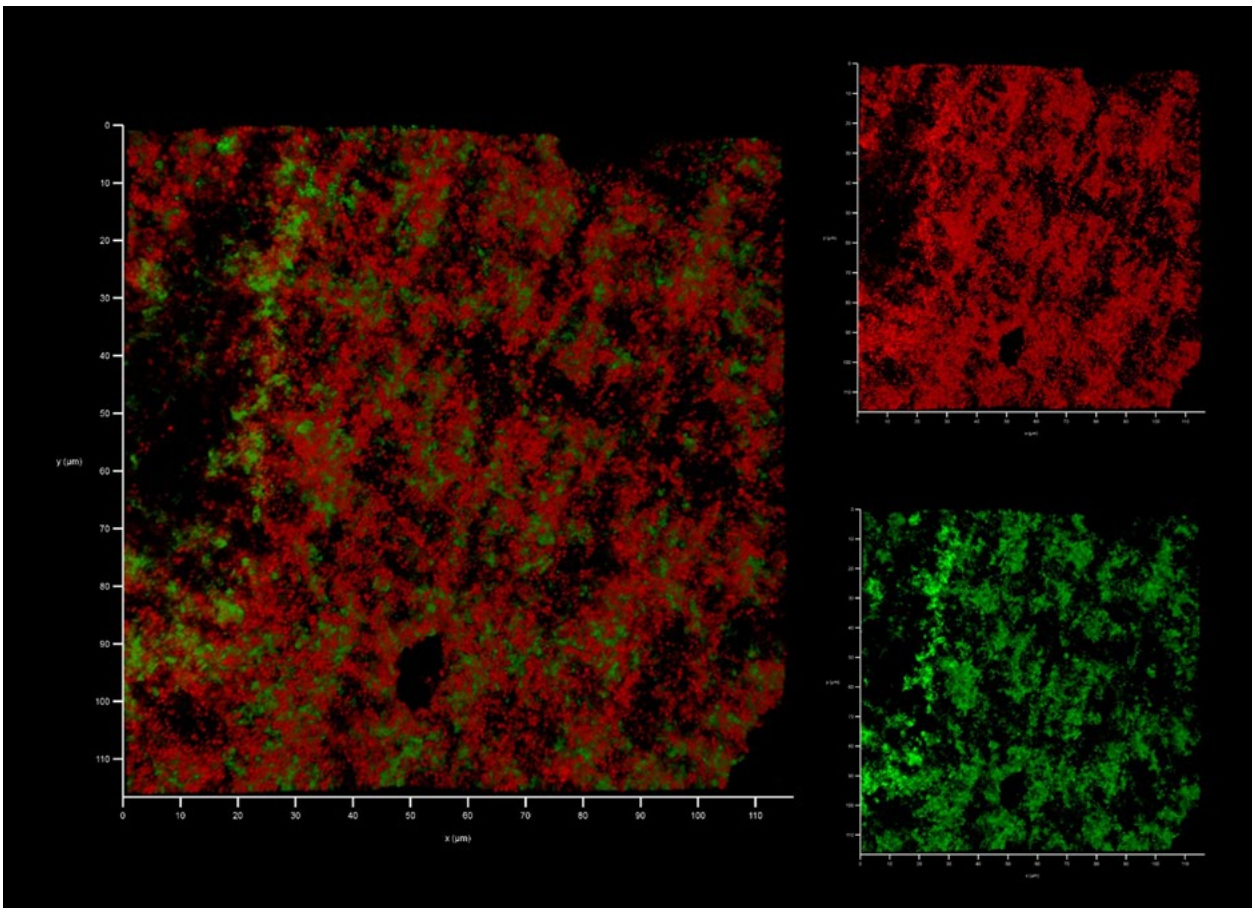

Fig. 3. CLSM visualization of three-day-old biofilm of *S.aureus* ATCC 25923, co-stained by Ethidium bromide (red) to visualize intracellular DNA, i.e. bacterial cells, and AmyGreen (green) to visualize functional amyloids in the biofilm matrix.

(Fig. 2). In order to compare the amyloid visualization in the biofilm, the co-staining with AmyGreen and Ethidium bromide was used (Fig. 3). The noticeable distinction between D-16 and SYBR Green localization was observed, indicating the structural separation of the biofilm components stained by D-16 and the cells stained by SYBR Green in the biofilm matrix. It shows that the dye does not penetrate bacterial cells and does not stain intracellular DNA, despite a high sensitivity of the dye to this biomolecule. The staining pattern of D-16 may correspond to the accumulation pattern of functional amyloids in the biofilm matrix. The accumulation mode corresponded to that observed in the control staining by AmyGreen (green signal) (Fig. 3). Thus, dye D-16 can be proposed as a red-yellow emitted probe to visualize the extracellular matrix of *S. aureus ATCC25923* biofilm.

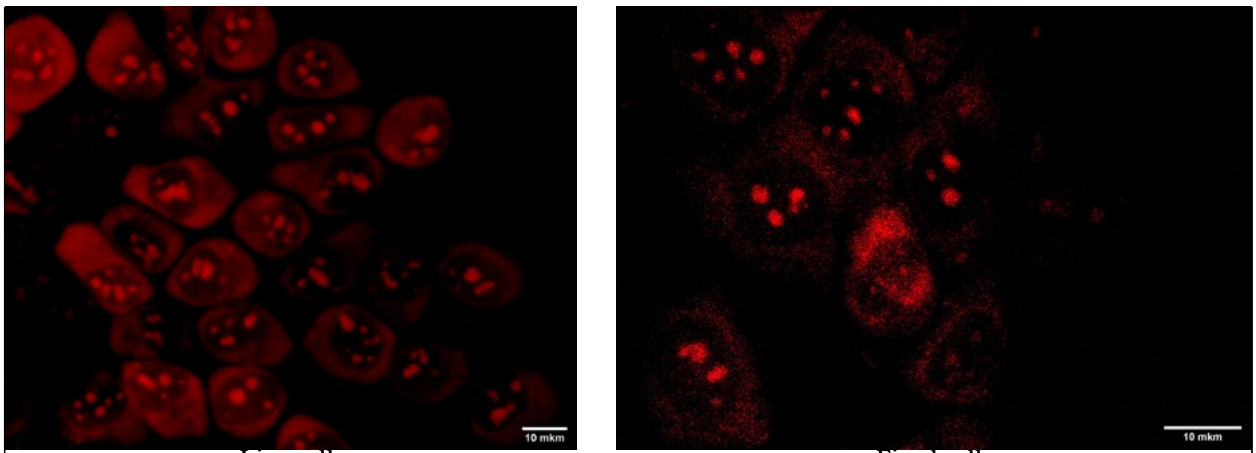

Fig. 4. Fluorescence image of visualization of MCF-7 cell line with styrylcyanine dye D-16 (C_{dye} = 10 μM). Scale bar — 10 μm.

Visualization of breast cancer cell line MCF-7 by styrylcyanine dye

To estimate the ability of the dye to penetrate eukaryotic cells and to stain intracellular components, the staining of human MCF-7 cells as the amyloid fibrils-free model was performed. It is seen from Fig.4 that D-16 can penetrate the cellular membrane and nucleus pores of the cells. Given the sensitivity of the dye to RNA, we can assume that the dye stains the RNA-containing components of the cell. A similar effect was previously shown for Thioflavin T [30]. Like Thioflavin T, D-16 stains RNA in cytoplasm, penetrates nuclei, and visualizes the components presumably nucleoli — the complex of proteins and ribonucleoproteins formed around DNA sites.

Conclusions

The amyloid-sensitive styrylcyanine dye D-16 is proposed as a green\yellow-emitting stain to visualize the extracellular matrix of bacterial biofilms. We studied *in vitro* the fluorescent sensitivity of this dye to different biomolecules, which are significant components of cells, EPS, or medium for cultivation: nucleic acids, polysaccharides, lipids, and proteins. The most significant spectral responses were observed for amyloid fibrils of BLG (214 times) following with DNA, RNA (102 and 191 times, respectively), and amyloid fibrils of lysozyme (108 times). Irradiation was performed to study the photostability of the dye. We observed an increase in the photostability of the dye bound to biomolecules and higher photostability with amyloid fibrils of BLG. The efficient visualization of amyloid-producing biofilm by styryl dye was explored on the model *S.aureus* ATCC 25923 bacteria biofilm. The noticeable distinction between D-16 and SYBR Green localization was observed, indicating the structural separation of the biofilm components stained by D-16 and the cells stained by SYBR Green in the biofilm matrix. It evidences that the dye does not penetrate bacterial cells and does not stain intracellular DNA, despite a high sensi-

tivity of the dye to this biomolecule. The staining pattern of D-16 corresponds to that obtained when AmyGreen was applied to the same biofilm. The above mentioned confirmed that the staining pattern of D-16 may correspond to the accumulation pattern of functional amyloids in the biofilm matrix.

The staining of human MCF-7 cells as an amyloid fibrils-free model was carried out to estimate the ability of the dye to penetrate eukaryotic cells and stain intracellular components. We have assumed that the dye stains the RNA-containing components of the MCF-7 cells (penetrates nuclei and visualizes ribonucleoproteins complexes - nucleoli) similarly to the amyloid-sensitive probe Thioflavin T, but with red emission.

Acknowledgments

S.C. and G.V. are grateful for the grant of a group of young scientists of NASU №0120U000079 for 2020–2021.

REFERENCES

1. *Koza A, Kusmierska A, McLauglin K, Moshynets O, Spiers AJ.* Adaptive radiation of P. fluorescens SBW25 in experimental microcosms provides an understanding of the evolutionary ecology and molecular biology of A-L interface biofilm-formation. *FEMS Microbiol Lett*. 2017;**364**(12).
2. *Moshynets OV, Spiers AJ.* Viewing biofilms within the larger context of bacterial aggregations. In "Biofilms". *InTech Press*, 2016; 3–22.
3. *Robertson M, Hapca SM, Moshynets O, Spiers AJ.* Air-liquid interface biofilm formation by psychrotrophic pseudomonads recovered from spoilt meat. *Antonie Van Leeuwenhoek.* 2013; **103**(1):251–9.
4. *De Rycker M, Horn D, Aldridge B, Amewu RK, Barry CE, Buckner FS, Cook S, Ferguson MA, Gobeau N, Herrmann J, Herrling P, Hope W, Keiser J, Lafuente MJ, Leeson PD, Leroy D, Manjunatha UH, McCarthy J, Mizrahi V, Moshynets O, Niles J, Overington JP, Pottage J, Rao SP, Read KD, Ribeiro I, Silver LL, Southern J, Spangenberg T, Sundar S, Taylor C, Voorhis WV, White NJ, Wyllie S, Wyatt PG, Gilbert IH.* Setting our sights on infectious diseases. *ACS Infectious Disease.* 2020; **6**(1):3–13
5. *Moshynets O, Bardeau JF, Tarasyuk O, Makhno S, Cherniavska T, Dzhuzha O, Potters G, Rogalsky S.* Antibiofilm activity of polyamide 11 modified with thermally stable polymeric biocide polyhexamethylene gua-nidine 2-naphtalenesulfonate.*Int J Mol.* Sci. 2019; **20**(2):348.
6. *Flemming H-C, Wingender J, Szewzyk U, Steinberg P, Rice SA, Kjelleberg S.* Biofilms: an emergent form of bacterial life. *Nat Rev Microbiol.* 2016;**14**(9): 563–75.
7. *Matz C, Kjelleberg S.* Off the hook—how bacteria survive protozoan grazing. *Trends Microbiol.* 2005;**13**(7):302–7.
8. *Lee KWK, Periasamy S, Mukherjee M, Xie C, Kjelleberg S, Rice SA.* Biofilm development and enhanced stress resistance of a model, mixed-species community biofilm. *ISME J.* 2014;**8**(4):894–907.
9. *Burmølle M, Ren D, Bjarnsholt T, Sørensen SJ.* Interactions in multiespecies biofilms: do they actually matter? *Trends Microbiol*. 2014; **22**(2):84–91.
10. *Young KD.* The selective value of bacterial shape. *Microbiol Mol Biol Rev.* 2006;**70**(3):660–703.
11. *Martin M, Hölscher T, Dragos A, Cooper VS, Kovács AT.* Laboratory evolution of microbial interactions in bacterial biofilms. *J Bacteriol.* 2016; **198**(19):2564–71.
12. *Moshynets OV, Foster D, Karakhim SA, McLaughlin K, Rogalsky SP, Rymar SY, Volynets GP, Spiers AJ.* Examining c-di-GMP and possible QS regulation in Pseudomonas fluorescens SBW25: links between intra and inter-cellular regulation benefits community cooperative activities such as biofilm formation. *Ukr Biochem J.* 2018; **90** (3): 17–31.
13. *Hobley L, Harkins C, MacPhee CE, Stanley-Wall NR.* Giving structure to the biofilm matrix: an overview of individual strategies and emerging

common themes. *FEMS Microbiol Rev.* 2015; **39**(5):649–69.

14. *Turnbull L, Toyofuku M, Hynen AL, Kurosawa M, Pessi G, Petty NK, Osvath SR, Cárcamo-Oyarce G, Gloag ES, Shimoni R, Omasits U, Ito S, Yap X, Monahan LG, Cavaliere R, Ahrens CH, Charles IG, Nomura N, Eberl L, Whitchurch CB*. Explosive cell lysis as a mechanism for the biogenesis of bacterial membrane vesicles and biofilms. *Nat Commun.* 2016; **7**:11220.
15. *McLaughlin K, Folorunso AO, Deeni YY, Foster D, Gorbatiuk O, Hapca SM, Immoor C, Koza A, Mohammed IU, Moshynets O, Rogalsky S, Zawadzki K, Spiers AJ.* Biofilm formation and cellulose expression by Bordetella avium 197N, the causative agent of bordetellosis in birds and an opportunistic respiratory pathogen in humans. *Res Microbiol.* 2017; **168**(5): 419–30.
16. *Dueholm MS, Otzen D, Nielsen PH.* Evolutionary insight into the functional amyloids of the pseudomonads. *PLoS One.* 2013;**8**(10):e76630.
17. *Serra D, Richter A, Klauck G, Mika F, Hengge R.* Cellulose as an architectural element in spatially structured Escherichia coli biofilms. *J Bacteriol.* 2013; **4**(2):e00103–13.
18. *Archer GL.* Staphylococcus aureus: a well-armed pathogen. *Clin Infect Dis.* 1998;**26**(5):1179–81.
19. *Pérez-Montarelo D, Viedma E, Murcia M, Muñoz-Gallego I, Larrosa N, Brañas P, Fernández-Hidalgo N, Gavaldà J, Almirante B, Chaves F.* Pathogenic characteristics of Staphylococcus aureus endovascular infection isolates from different clonal complexes. *Front Microbiol.* 2017;**8**:917.
20. *Cucarella C, Solano C, Valle J, Amorena B, Lasa I, Penadés JR.* Bap, a Staphylococcus aureus surface protein involved in biofilm formation. *J Bacteriol.* 2001;**183**(9):2888–96.
21. *Van Gerven N, Van der Verren SE, Reiter DM, Remaut H.* The role of functional amyloids in bacterial virulence. *J Mol Biol.* 2018;**430**(20):3657–84.
22. *Volynets G, Vyshniakova H, Nitulescu G, Nitulescu GM, Ungurianu A, Margina D, Moshynets O, Bdzhola V, Koleiev I, Iungin O, Tarnavskiy S, Yarmoluk S.* Identification of novel antistaphylococcal hit compounds targeting Sortase A. *Molecules.* 2021;**26**(23):7095.
23. *Kim JY, Sahu S, Yau YH, Wang X, Shochat SG, Nielsen PH, Dueholm MS, Otzen DE, Lee J, Delos Santos MM, Yam JK, Kang NY, Park SJ, Kwon H, Seviour T, Yang L, Givskov M, Chang YT.* Detection of pathogenic biofilms with bacterial amyloid targeting fluorescent probe, CDy11. *J Am Chem Soc.* 2016;**138**(1):402–7.
24. *Otzen D.* Functional amyloid: turning swords into plowshares. *Prion.* 2010;**4**(4):256–64.
25. *Oli MW, Otoo HN, Crowley PJ, Heim KP, Nascimento MM, Ramsook CB, Lipke PN, Brady LJ.* Functional amyloid formation by Streptococcus mutans. *Microbiology.* 2012;**158**(Pt 12):2903–16.
26. *Shewmaker F, McGlinchey RP, Wickner RB.* Structural insights into functional and pathological amyloid. *J Biol Chem.* 2011;**286**(19):16533–40.
27. *Sugimoto S, Arita-Morioka K, Mizunoe Y, Yamanaka K, Ogura T.* Thioflavin T as a fluorescence probe for monitoring RNA metabolism at molecular and cellular levels. *Nucleic Acids Res.* 2015;**43**(14):e92.
28. *Kovalska V, Chernii S, Losytskyy M, Dovbii Y, Tretyakova I, Czerwieniec R, Chernii V, Yarmoluk S, Volkov S.* β-ketoenole dyes: synthesis and study as fluorescent sensors for protein amyloid aggregates. *Dyes Pigments.* 2016;**132**:274–81.
29. *Kovalska V, Chernii S, Losytskyy M, Tretyakova I, Dovbii Y, Gorski A, Chernii V, Czerwieniec R, Yarmoluk S.* Design of functionalized β-ketoenole derivatives as efficient fluorescent dyes for detection of amyloid fibrils. *New J Chem.* 2018; **42**(16): 13308–18.
30. *Moshynets O, Chernii S, Chernii V, Losytskyy M, Karakhim S, Czerwieniec R, Pekhnyo V, Yarmoluk S, Kovalska V.* Fluorescent β-ketoenole AmyGreen dye for visualization of amyloid components of bacterial biofilms. *Methods Appl Fluoresc.* 2020; **8**(3): 035006.
31. *Mazaheri M, Moosavi-Movahedi AA, Saboury AA, Khodagholi F, Shaerzadeh F, Sheibani N.* Curcumin protects β-Lactoglobulin fibril formation and fibril-induced neurotoxicity in PC12 Cells. *PLoS One.* 2015;**10**(7):e0133206.

32. *Kovalska V, Chernii S, Cherepanov V, Losytskyy M, Chernii V, Varzatskii O, Naumovets A, Yarmoluk S.* The impact of binding of macrocyclic metal complexes on amyloid fibrillization of insulin and lysozyme. *J Mol Recognit.* 2017; **30**(8):e2622.
33. *Sambrook J, Fritsch E, Maniatis T.* Molecular Cloning: A Laboratory Manual (2nd ed.*).* Cold Spring Harbor, NY: Cold Spring Harbor Laboratory Press. 1989.
34. *Schindelin J, Arganda-Carreras I, Frise E, Kaynig V, Longair M, Pietzsch T, Preibisch S, Rueden C, Saalfeld S, Schmid B, Tinevez JY, White DJ, Hartenstein V, Eliceiri K, Tomancak P, Cardona A.* Fiji: an open-source platform for biological-image analysis. *Nat Methods.* 2012;**9**(7):676–82.

Бензоксазольний стирилціаніновий барвник як флуоресцентний зонд для візуалізації функціональних амілоїдів у біоплівці *Staphylococcus aureus* ATCC25923

С. В. Черній, О. В. Мошинець, Д. І. Арістова,
Д. В. Криворотенко, М. Ю. Лосицький,
О. С. Юнгін, С. М. Ярмолюк, Г. П. Волинець

Мета. Синтез та характеристика стирилціанінового барвника як потенційного флуоресцентного зонда для виявлення патологічних амілоїдних фібрил *in vitro* та виявлення функціонального амілоїду в біоплівці *S. aureus*. **Методи.** Хімічний синтез, флуоресцентна спектроскопія, вивчення фотостабільності опроміненням джерелом видимого світла, конфокальна мікроскопія, флуоресцентна мікроскопія. **Результати.** Стирилціаніновий барвник у вільному стані має низькоінтенсивну флуоресценцію, але в присутності амілоїдних фібрил *in vitro* показує збільшення інтенсивності емісії до 214 разів залежно від структури амілоїдогенного білка, найбільш виражене підвищення спостерігалося для фібрил бета-лактоглобуліну. Фотостабільність барвника у вільному стані низька, але зв'язування з амілоїдними фібрилами призводить до сильного збільшення фотостійкості барвника. Після фарбування біоплівки *S. aureus* барвник забарвлює позаклітинні компоненти матриксу біоплівки і не проникає у клітину. Висновок. Цей барвник запропоновано для візуалізації функціональних амілоїдів біоплівки *S. aureus* у червоному спектрі.

Ключові слова: флуоресцентна мікроскопія, стирилові барвники, *S.aureus*, функціональні амілоїди, бактеріальна біоплівка, конфокальна лазерна скануюча мікроскопія.

Бензоксазольний стирилцианиновий краситель как флуоресцентный зонд для визуализации функциональных амилоидов в биопленке *Staphylococcus aureus* ATCC25923

С. В. Черний, Е. В. Мошинец, Д. И. Аристова,
Д. В. Криворотенко, М. Ю. Лосицкий,
О. С. Юнгин, С. Н. Ярмолюк, Г. П. Волинец

Цель. Синтез и характеристика стирилцианинового красителя как потенциального флуоресцентного зонда для выявления патологических амилоидных фибрилл *in vitro* и выявления функциональных амилоидов в биопленке *S. aureus*. **Методы.** Химический синтез, флуоресцентная спектроскопия, изучение фотостабильности облучением источником видимого света, конфокальная микроскопия, флуоресцентная микроскопия. **Результаты.** Стирилцианиновий краситель в свободном состоянии имеет низкую флуоресценцию, но в присутствии амилоидных фибрилл *in vitro* показывает увеличение интенсивности эмиссии до 214 раз в зависимости от структуры амилоидогенных белка, наиболее выраженное повышение наблюдалось для фибрилл бета-лактоглобулина. Фотостийкисть красителя в свободном состоянии низкая, но связывания с амилоидными фибриллами приводит к сильному увеличению фотостабильности красителя. После окрашивания биопленки *S. aureus* краситель визуализирует внеклеточные компоненты матрикса биопленки и не проникает в клетку. Вывод. Этот краситель предложено для визуализации функциональных амилоидов биопленки *S. aureus* в красном спектре.

Ключевые слова: флуоресцентная микроскопия, стириловые красители, *S.aureus*, функциональные амилоиды, бактериальная биопленка, конфокальная лазерная сканирующая микроскопия.

Received 05.09.2021